QUANTITATIVE DETERMINATION OF LITHOFACIES USING GEOPHYSICAL INVERSE THEORY, DRINKARD UNIT, PERMIAN BASIN, LEA CO., N.M.

Ata Sagnak, Texaco E&P, Midland, TX
Harold Gurrola and George Asquith
Texas Tech University, Lubbock, TX

ABSTRACT

The determination of the correlation between petrophysical data, and core data is essential in the determination of reservoir rock properties. The goal of this study was to design a computer algorithm, which will use the geophysical inverse theory to deduce different reservoir facies, from well log responses, **by** utilizing statistical relationships between the well logs and core derived lithofacies information.

In most oil and gas fields only a minority of the wells are cored. As a result, determination of reservoir rock properties is mainly dependent on the interpretation of geophysical log data. An objective approach to analyze well log data to determine the reservoir rock properties, would speed up the interpretive process and would also enable the researcher to correlate information between wells and incorporate a-priori knowledge into their interpretation.

Detailed core and petrographical analysis was conducted as the first step in establishing statistical relationships of lithological data from four cored wells. Petrographically sixteen major rock types (lithofacies) were identified. Secondly, a valid forward model, which is a requirement in any successful inversion process, was constructed by the usage of mathematical formulation of well logs, and the petrographical data obtained from cores. Well logs used for this study include Neutron, Spectral Density including Bulk Density and Photoelectric Absorption Index (Pe), and Borehole Compensated Sonic (Interval Transit Time) logs. A unity constraint was also used as a supplementary log data. Thirdly, an inversion method, which can incorporate the results of core analysis and petrographical information as a-priori geologic information, as potential constrains in the inversion itself was determined.

The facies observed between wells in a given oil and gas field are related to each another. Therefore, using the a-priori information from the cored wells, with reservoir facies control, to determine if results from selected well(s) can provide lithofacies information in the remaining wells would improve the reservoir management efforts. An inversion algorithm, using a-priori geologic information was tested on four cored wells.

Inversion method was tested for different a-priori geologic information cases where the examined facies were grouped in sixteen, fourteen, eleven, and five lithofacies classes. The robustness of the inversion results was found to depend on the a-priori information provided. Lithofacies inversion, using five lithofacies classes, showed reliable estimations for the purpose of depicting possible reservoir versus non-reservoir zones. The method used was also able to reliable identify most of the eleven facies classes. Inversion, using sixteen and fourteen different facies, showed to be a valuable tool in determining the gross lithology.

INTRODUCTION

The focus of this study, the lower Leonardian Drinkard unit, in the West Dollarhide Field of Central Basin Platform of Permian Basin, is an economically important oil producer (Figure 1) and is associated with the lower Leonardian Abo formation (Figure 1). Detailed core and petrographical analysis is the first step in establishing statistical relationships between core and well log data. Secondly, it is necessary to construct a valid forward model, a requirement in any successful inversion process. Thirdly, an inversion method, which incorporates the results of core analysis and petrographical information (a-priori geologic information) as constraints has to be determined. The emphasis in this study is strictly on the inversion method. The core analysis and petrographical findings of this study are used for identifying different reservoir facies and are not intended as the interpretations of depositional environments.

REGIONAL GEOLOGY AND STRATIGRAPHY

West Dollarhide Field is located in Lea County, New Mexico and is the western extension of the Dollarhide Field in

Andrews County, Texas (Figure 1). The Leonardian rocks in the Central Basin Platform, constitute a thick, highly cyclic succession of shallow platform carbonates. The Drinkard unit in the West Dollarhide Field was deposited in an inner-ramp environment. Inner-ramp deposits contain a thick, highly cyclic succession of carbonate rocks, some anhydrite, minor amounts of interbedded siliciclastic sandstones, and siltstone of primarily eolian origin (Ruppel, 1992). These rocks exhibit highly variable shallow-water subtidal to tidal-flat facies assemblages. Subtidal rocks include skeletal and pellet packstones and mudstones. The tidal-flat rocks consist of a broader extent of depositional textures that are locally silty and clay rich. They also include fenestral and stromatolitic limestone to wackestone and peloidal mudstone. The heterogeneity in the inner-ramp rocks primarily results from the stacking of different facies on top each other as well as postdepositional diagenesis (Ruppel and others, 1995).

GENERALIZED INVERSE THEORY

Generalized inverse theory provides techniques for solving systems of linear equations. The linear equations can be of any size, and the number of equations may be less than, the same as, or greater than the number of the unknown (Smith and Franklin, 1969). Linear algebraic equations can also be expressed by matricies, and such equations can be solved by matrix inversion utilizing generalized inverse method. In a given equation similar to below, the solution of $|M|$ would require the multiplication of both sides of the equation by the inverse matrix $|X|^{-1}$. The solution for $|M|$ then would be as follows (Doveton, 1994, Hoffman, 1992, Davis, 1986, Doveton and Cable, 1979).

$$|Y| = |X|\,|M| \quad (1)$$

$$|X|^{-1}|Y| = |X|^{-1}|X|\,|M| \quad (2)$$

$$\text{since: } |X|\,|X|^{-1} = |I| \text{ and } |I|\,|M| = |M| \quad (3)$$

$$|X|^{-1}|Y| = |M| \quad (4)$$

In the equations above, $|X|$ is a matrix of component log properties, $|M|$ is a vector of unknown proportions of rock components or unknown model parameters, and $|Y|$ is a vector of log responses of the zone of interest. The given equation can be interpreted as specifying a linear model describing the relationship between log measurements and rock properties thus representing an inverse problem. In other words, the rock composition (M or model parameters) is deduced from its physical properties by utilizing the well log measurements. On the other hand, prediction of log measurements from known rock composition and proportions represents a forward problem. For simplicity, matricies from now on will be represented by a capital letter (ie: M, instead of $|M|$).

METHODS OF RESEARCH

Research methods dealing with the direct study of Drinkard unit includes detailed core description and petrographic analysis. The findings of core description and petrographic analysis were used to subdivide the studied interval into different lithological facies. Texaco E&P Inc. granted permission to study four cored wells located in Townships 24-S and 25-S, and Range 38-E in the West Dollarhide Field in Lea County, New Mexico. Due to the confidentiality of the data from these wells, the cores will be referred to as core 1, core 2, core 3, and core 4 (Figure 2). The available cores were logged in detail by using standard visual logging techniques. Each core was divided into distinct lithlogical zones based on their distinct lithological characteristics obtained from core analysis and petrographic analysis for every half-foot interval, which is also the resolution of well log data. Second source of information from the cores came from the results of Core Analysis Report provided by Texaco E&P Inc. Helium porosity measurements of the core analysis were used as the primary source for porosity values for each zone.

Petrographic analysis was used in determining the lithofacies and the findings were incorporated into the data obtained from visual core analysis in order to have a continuous coverage throughout the studied wells. In each thin section, percentages of dolomite, calcite, anhydrite, shale, and pore space were determined by both point count and visual area percentage estimation methods. The compositional values from the thin section analysis were incorporated with the well log data and core data.

Dunhman (1962) classification of carbonate rocks was used to assign different facies names (lithofacies) to each lithology. Four major lithological groups were observed in the thin sections. They include dolomites, dolomitized limestones, dolomitic limestones, and limestones. The forty-one lithofacies observed were originally classified into sixteen major lithofacies groupings. This classification was then modified into fourteen, eleven, and five lithofacies classifications by grouping lithologically similar facies into similar classes. Inversion method was tested on each lithofacies class to test the robustness of the algorithm. The list of the lithofacies classes and each lithofacies is given in the appendix.

Neutron porosity (NPHI), Spectral Density or Formation Bulk Density (RHOB), Interval Transit Time or Sonic (ITT or D t). and Photoelectric Absorption Index (Pe) curves provided the petrophysical data for this study. These log types

were chosen solely due to their linear or curvilinear character in their response equations. The resolution of well log data was chosen as the necessary resolution for the inversion algorithm. For that reason, the petrographic data and the core analysis report data (mainly, the He-porosity values) were extrapolated to every half-foot interval in an attempt to match the resolution of well log data. It should be noted here that the term "resolution" is intended to represent the frequency of data points or the sampling interval.

FORWARD MODEL

In this study, inversion is defined as constructing an earth model from available log data. **A** perquisite for a successful inversion, is to construct a valid forward model although a valid forward model does not guarantee a successful inversion. The first step in testing the results of any inversion method is to test the forward model, from where the desired parameters are to be inverted. For this study, principal aim of constructing a forward model is to obtain synthetic well logs by using actual rock parameters. The parameters used in forward model include depth, percentages of each major constituent forming the rock (dolomite, calcite, anhydrite, shale, pore space or fluid), and log response values of each constituent forming the rock. Once a forward model is successfully achieved, inversion can be attempted in order to generate an earth model from log data

Constituents of forward model can also be used to provide means of verifying solutions to an inverse problem. The difference between the observed well log measurements and values calculated by the forward model, can be used as an indicator of misfit or error. Improvements to the component parameters and tool response equations can be done if there is a large difference between the synthetic logs and actual measured logs. During the development of the forward model used in this study, this aspect was taken into account and the constituent parameters were modified. The magnitude of misfit, or error, can be used to quantify the validity of any inversion result. The misfit can also be used as a constraint. which is minimized in the inversion.

The forward model in this study consists of log responses of Compensated Neutron Log (CNL), Bulk Density Log (Rho-b Log), Interval Transit Time (ITT-log), and Photoelectric Absorption Index (Pe-Log). The response equations of these logging tools as used in this study are in the appendix. Figure 3 is an example for testing the validity of the forward model where the plots of calculated well log (forward model or synthetic log) and measured well log responses are plotted for neutron log.

The first step in the integration of well log data with the core data is to establish a correct depth match for both sources of information. Commonly, core depths are matched with well log depths by comparing the available curves from both sources. The initial depth shifts used by earlier researchers were considered correct because of no apparent reason not to believe so. Inversion algorithm was then applied to various lithologies in all of the wells.

Synthetic logs were then compared with the measured logs and some intervals appeared to be inadequately or wrongly shifted. This comparison showed significant differences (error) in the measured and synthetic log values at certain depths. **A** majority of the error occurred in the vicinity of depths where some intervals in the cores were labeled as missing. Comparing the measured and synthetic log curves, it was inferred that the errors were predominantly caused by wrong depth shifting of the core where it was labeled as missing. Further analysis resulted in the modified depth shift values for the examined cores. Figures 3 and 4 are the plots of neutron log using modified and unmodified depth shift for core 3 respectively.

Detailed and correct depth shifting is especially important in carbonate reservoirs like Drinkard unit, where the best reservoir intervals are usually thin. In the studied cores, the maximum thickness for possible best reservoir interval is about 7 ft. and the cores rarely exhibit reservoir facies intervals that are thicker than 6 ft. The usage of synthetic logs, as a tool in determining the amount of necessary depth shift could greatly benefit production in thin and/or alternating zones of reservoirs.

INVERSION METHOD

The method of well log inversion discussed here employs a two-step inversion to arrive at lithofacies information (constituent percentages). The forward model for this problem includes the generation of tool responses from known lithology and constituent tool parameters. Standard values for the constituents were taken from the logging company manual (Halliburton, 1994). The calculated (synthetic) responses of the studied tools using standard values indicated a need for the modification of the constituent tool parameters. So, an inversion method to invert for the constituent tool parameters is employed as the first step.

The response of each logging tool can be expressed in a form that represents a linear inverse problem by the equation:

$$R = P\,S, \tag{5}$$

where R is the log response of each logging tool at a given depth, P is the percentages of the constituents at a given depth, and S is the logging tool parameter of each constituent for the given logging tool. R is the $1 \cdot 1$ matrix composed of the log responses of NPHI, RHOB, ITT, or Pe logs as well as the unity constraint. P is a $1 \cdot 5$ matrix, and S is a $5 \cdot 1$ matrix. The following is an example for the Pe log at a given depth where R, **P,** and S are expressed as matrix forms:

$$R_1 = \left[Pe_1 \right], \tag{6}$$

$$P_1 = \left[dol_1 \quad ca_1 \quad anh_1 \quad shale_1 \quad pore_1 \right], \tag{7}$$

$$S, = \begin{bmatrix} Pe_{dol} \\ Pe_{ca} \\ Pe_{anh} \\ Pe_{shale} \\ Pe_{pore} \end{bmatrix} \tag{8}$$

where Pe_1 is the Pe response at depth (1), dol,, ca,, anh,, shale,, and pore, are the percentages of the constituents at depth (1), and Pe_{dol}, Pe_{ca}, Pe_{anh}, Pe_{shale}, Pe_{pore} are the constituent Pe tool parameters.
To extend this method for simultaneous inversion of **S,** for n number of depths the eq. 5 can be written as:

$$\begin{bmatrix} R_1 \\ R_2 \\ \vdots \\ R_n \end{bmatrix} = \begin{bmatrix} P_1 \\ P_2 \\ \vdots \\ P_n \end{bmatrix} \text{ S or } \boldsymbol{R} = P\,S, \tag{9}$$

where $\boldsymbol{R} = \begin{bmatrix} R_1 \\ R_2 \\ \vdots \\ R_n \end{bmatrix}$, $P = \begin{bmatrix} P_{1dol} & P_{1ca} & P_{1anh} & P_{1shale} & P_{1pore} \\ P_{2dol} & \text{Par.} & P_{2anh} & P_{2shale} & P_{2pore} \\ \vdots & & & & \vdots \\ P_{Ndol} & P_{Nca} & P_{Nanh} & P_{Nshale} & P_{Npore} \end{bmatrix}$ and $\boldsymbol{S} = \begin{bmatrix} S_{dol} \\ S_{ca} \\ S_{anh} \\ S_{shale} \\ S_{pore} \end{bmatrix}$

Equation 1 provides a theoretical response for a hypothetical lithology. **As** in the case of similar inversions (e.g., Gurrola and others 1995), noise is present in the observed R term (R_o) and an exact solution of eq. 5 would overfit the theoretical (R_t) response. **A** solution, in which the root mean square (rms) difference between the R_o and R_t is minimized, is therefore desired. The difference between the theoretical and observed data is defined as the misfit u.

$$u = (R_{theoretical} - R_{observed}) \text{ or } u = (R_t - R_o) \tag{10}$$

A set of tool parameters **S,** which minimizes u^2, in the following equations is therefore sought.

$$u^2 = (R_{o\text{-}i} - R_{t\text{-}i})^2 \tag{11}$$

$$u^2 = (\mathbf{P\,S} - \mathbf{R})^2 \tag{12}$$

In the presence of noise in R_o, a solution for **S** will be non-unique. Introduction of a particular constraint, and finding a solution for R, which satisfies the particular constraint helps stabilize the solution where the goal is to find R that is within noise level. Because the standard tool (manufacturer) parameters are close to the expected inverted tool param-

eters, an additional constraint is introduced. In this study, the difference between the standard tool parameters and the inverted tool parameters is used as a constraint, which is also referred to as the penalty function v.

$$v^2 = (S - S_{ref})^2. \quad (13)$$

By multiplying the eq. 13, with a Lagrange multiplier (l), and adding equations 12 and 13, a trade-off between the misfit u, and the penalty function v, that stabilizes the effect of noise is achieved.

$$u^2 + v^2 = (P\ S - R)^2 + \lambda\ (S - S_{ref})^2. \quad (14)$$

A local minimum can be found by differentiating the eq. 14 with respect to S and setting the results to zero (Gurrola and others, 1995).

$$\partial / \partial_S\ [u^2 + v^2] = a\ / \partial_S\ [\ (P\ S - R)^2 + \lambda\ (S - S_{ref})^2\ ]. \quad (15)$$

Solution for S then would be:

$$0 = P'\ (P\ S - R) + \lambda\ I\ (S - S_{ref}) \quad (16)$$

$$0 = P'\ P\ S - P'\ R + \lambda I\ S - \lambda_1\ I\ S_{ref} \quad (17)$$

$$S = (P'\ P + \lambda\ I)^{-1}\ (P'\ R + I\ S\lambda_{ref}) \quad (18)$$

where I is the 5 ' 5 identity matrix, l is the Lagrange multiplier, S_{ref} is the 5 ´ 5 standard tool parameter matrix, exponent ($^{-1}$) represents the inverse matrix, and (') represents the transpose matrix. In order to extend this method for the simultaneous inversion of S for n-number of depths where ***R, and*** P are as defined by eq. 9, would yield,

$$S = (\boldsymbol{P'\ P} + \lambda\ \ I)^{\prime}\ (P'\ R + \lambda\ I\ S_{ref}). \quad (19)$$

Due to the presence of noise in R an exact solution to eq. 1 is not expected. **A** Lagrange multiplier is used to input some degree of bias to the inverted values by favoring the standard tool parameters. The value of controls the degree to which the inversion is, controlled by S_{ref}. When g = 0, the inversion yields S which is unaffected by S_{ref}. **A** large value for g would result in the case where $S = S_{ref}$. **An** appropriate Lagrange multiplier λ , is selected on the basis of a compromise between heavy bias and no bias.

Once the appropriate tool parameters are selected, the next step is to apply an inversion method in an attempt to determine lithofacies. The derivation of this method is similar to the one described above and uses the same linear logging tool equations. **A** linear model describing the relationship between log measurements and rock properties at a given depth, which together represents an inverse problem can be defined by the matricies:

$$Y = \begin{bmatrix} NPHI_1 \\ RHOB_1 \\ ITT_1 \\ Pe_1 \\ 1 \end{bmatrix}, \quad (20)$$

$$X = \begin{bmatrix} NPHI_{dol} & NPHI_{ca} & NPHI_{ank} & NPHI_{shale} & NPHI_{pore} \\ RHOB_{dol} & RHOB_{ca} & RHOB_{ank} & RHOB_{shale} & RHOB_{pore} \\ ITT_{dol} & ITT_{ca} & ITT_{ank} & ITT_{shale} & ITT_{pore} \\ Pe_{dol} & Pe_{ca} & Pe_{ank} & Pe_{shale} & Pe_{pore} \\ 1 & 1 & 1 & 1 & 1 \end{bmatrix}, \quad (21)$$

$$M = \begin{bmatrix} \%_{dol} \\ \%_{ca} \\ \%_{anh} \\ \%_{shale} \\ \%_{pore} \end{bmatrix} \quad (22)$$

where, Y is the log response of each logging tool at depth (1), X is a matrix of constituent tool parameters, and M is a vector of unknown proportions of rock components, or unknown model parameters (percentages of dolomite, calcite, anhydrite, shale, and pore space) at depth (1). $NPHI_1$, $RHOB_1$, ITT_1, and Pe_1 are the corresponding tool responses at a given depth. $NPHI_{dol}$, $RHOB_{dol}$, ITT_{dol}, and Pe_{dol} are the tool parameters for mineral dolomite, and the same terminology applies to ca, anh, shale, and pore where each abbreviation refers to calcite, anhydrite, shale, and porosity respectively. The model parameter M, is represented by the percentages of dolomite, calcite, anhydrite, shale, and porosity and are represented by $\%_{dol}$, $\%_{ca}$, $\%_{anh}$, $\%_{shale}$, and $\%_{pore}$, respectively.

Collectively eqs. 20, 21, and 22 can be expressed as:

$$Y = X\ M. \quad (23)$$

Similar to the previous example, difference between the observed (Y_o) data and the theoretical **(Y,)** data, referred to as the misfit u.

$$u = (Y_{theoretical} - Y_{observed}) \text{ or } u = (Y_t - Y_o). \quad (24)$$

A solution, in which the root mean square (rms) difference between the R_o and R_t, (misfit) is minimized is therefore sought.

$$u^2 = (X\ M - Y)^2. \quad (25)$$

Each of the lithofacies discussed earlier, can also be represented by a standard (average) model parameter M_{ref}, as defined by the different lithofacies classifications. **A** penalty function v, is defined as the difference between the inverted M and M_{ref} and controls the degree of deviation of the inverted percentages from the average percentages and is expressed as:

$$v^2 = (M - M_{ref})^2. \quad (26)$$

Another penalty function w, is defined as the first derivative norm of the model parameter M, which forces the elements of M to be similar to each other and is defined as:

$$w^2 = (D\ M)^2. \quad (27)$$

where D is the derivative matrix of:

$$D = \begin{bmatrix} 1 & -1 & 0 & 0 & 0 & 0 \\ 0 & 1 & -1 & 0 & 0 & \\ 0 & 0 & 1 & -1 & 0 & \\ 0 & 0 & 0 & 1 & -1 & 1 \\ -1 & 0 & 0 & 0 & 1 & \end{bmatrix} \quad (28)$$

By multiplying the eq. **17** with a Lagrange multiplier l_1, and the eq. 18 with Lagrange multiplier l_2, and adding both equations to the eq. 16, a trade of between the misfit and the constraints can be achieved.

$$u^2 + v^2 + w^2 = (X\ M - Y)^2 + l_1 (M - M_{ref})^2 + l_2 (D\ M)^2. \quad (29)$$

An ideal solution would be where both u and v are minimized. By differentiating the eq. 29 with respect to M and setting the result to zero, the term $u^2 + v^2 + w^2$, is minimized while satisfying all the constraints and obtaining a stable value for M.

$$\partial / \partial_M [u^2 + v^2 + w^2] = \partial / \partial_M [(X\ M - Y)^2 + l_1 (M - M_{ref})^2 + l_2 (D\ M)^2]. \quad (30)$$

Solution for **M** then would be:

$$0 = X' (X M - Y) + \lambda_1 I (M - M_{ref}) + \lambda_2 D' (D M), \quad (31)$$

$$0 = X' X M - X' Y + \lambda_1 I M - \lambda_1 I M_{ref} + \lambda_2 D' D M, \quad (32)$$

$$M = (X' X + \lambda_1 I + \lambda_2 D' D)^{-1} (X' Y + \lambda_1 I M_{ref}). \quad (33)$$

where, I is the identity matrix and transpose matrix is represented by the apostrophe (i.e., X').

To extend this method for the simultaneous inversion of M, for more than one depth, the eq. 23 can be written **as:**

$$\begin{vmatrix} Y_1 \\ Y_2 \\ \\ Y_n \end{vmatrix} = X \begin{vmatrix} M_1 \\ M_2 \\ \vdots \\ M_n \end{vmatrix} \quad \mathbf{S} \text{ or } \boldsymbol{Y} = X M. \quad (34)$$

or, the simultaneous inversion of M for n-number of depths where ***Y and*** X are as defined by eq. 34, would be ,

$$M = (X' X + \lambda_1 z + \lambda_2 D' D)^{-1} (X' Y + \lambda_1 I M_{ref}). \quad (35)$$

Lagrange multipliers were used to control the effectiveness of each constraint by assigning different values to them. Lagrange multiplier one, l_1, is applied to the penalty function v, where the a-priori geological information is introduced $(M - M_{ref})$. The value of l_1 controls the degree of geologic bias applied to the inversion of M for each depth. M_{ref} is a matrix containing the reference rock types, or lithofacies, as defined by detailed core examination and petrographical study (lithofacies classifications).

The appropriate values for 1, and l_2 are determined by comparing the values of l_1 and l_2, which satisfy the constraints v and w (eqs. 26 and 27) in the minimization of misfit and constraint v. Zones with known lithologies were inverted for the values of l_1 and l_2 ranging from zero to one, and the results were plotted. Plots using different lithofacies classes, suggested similar minimum values for the Lagrange multipliers and 0.1 and 0.03 were selected as l_1 and 1, respectively that represents appropriate values for every lithofacies..

The selection criteria for the lithofacies inversion, **is** based on both the misfit u, and the penalty function v. The inversion result for M at each depth is compared with the lithofacies classification M_{ref}, in order to find a match between the inverted (M) and the reference (M_{ref}) based on a pre-defined tolerance. If there is not a match within the given limits of tolerance, the value of l, is increased in order to force the inversion to favor one of the lithofacies classes provided as reference. This process is repeated until an appropriate match is found. The value for l_1 is chosen as the smallest possible value, where the results in u and v are consisted with error introduced by the petrographic analysis (i.e., ± 3-4%). The small value of Lagrange multiplier l„ applied to constraint w, has little effect on the result of the lithofacies inversion.

RESULTS AND DISCUSSION

The sixteen initial lithofacies were observed in the examined cores. Petrophysically, depiction of sixteen different lithofacies from well logs is unrealistic and unexpected due to the insensitivity of logs to most of the physical characteristics that distinguish these lithofacies from each other. For example, as far as the well logs are concerned, there is little to no difference between a sucrosic dolomite and a dolomitized grainstone with similar porosity. This provided the basis for the re-classification of the initial sixteen facies. Each classification is based on whether different facies could be identified from well logs only using a lithofacies inversion method, and petrophysically similar facies are grouped together. The lithofacies classification for all four cases is included in Appendix .

The results of the lithofacies inversion method for each core are presented in five different plots. Figures 5, 6, 7, 8 and 9 display these results for core 4. Figure 5 has six sub-plots and is composed of the plots of the inverted and core derived percentages of dolomite, calcite, anhydrite, shale and pore space. Besides core porosity (He-porosity), Neutron-Density cross plot porosity was also used in the plots in order to see the relationship between the inverted and log derived porosity.

In each of the sub-plots in figure 5, the x-axis represents constituent percentages including core and log derived porosities. From left to right, the sub-plots represent inversion results (M) for dolomite, calcite, anhydrite, shale, He-porosity, and Neutron-Density cross plot porosity. The inverted values are shown in red and the core/log-derived values are shown in blue. Inverted porosity is plotted against both He-porosity and cross plot porosity in order to compare the

results for each case. Figure 5 is obtained by using the lithofacies inversion method utilizing sixteen classes as a-priori geologic information (M_{ref}).

Figure 6 is also obtained by the application of lithofacies inversion method utilizing sixteen classes and is composed of three sub-plots and contains the plots of Lagrange multiplier used by the inversion, inverted and core determined lithofacies, and combination of inverted constituent percentages. Y-axis in each sub-plot represents depth and except the combination inverted constituent percentage plot, red curves represent the result of the inversion algorithm and blue curves represent values obtained from either petrographic analysis, core analysis, or well log cross plot values. First sub-plot of Figure 8 represents the value of Lagrange multiplier λ_l and x-axis represents the value of λ_l. Second sub-plot compares the inverted and core derived lithofacies and the x-axis corresponds to the lithofacies number as defined by the classifications using sixteen, fourteen, eleven, and five classes. The last sub-plot is similar to Figure 7 but the inverted constituent values are shown on the same plot where the x-axis represents the percentages of each constituent.

Figure 7 is obtained by applying the lithofacies inversion method to core 4 where the a-priori geologic information included fourteen facies classes. Figures 8 and 9 display the inversion results for the cases of eleven and five lithofacies classes, respectively. The Lagrange multiplier λ_l values for the inversion results using different lithofacie classifications show little difference for each case and are not shown. Where the inversion result **(M),** is within the given tolerance to the reference facies classification (M_{ref}), the λ_l values are small. Higher λ_l values are observed where the M does not match the input M_{ref} values and λ_l was increased until the tolerance criteria, was matched. Inversion results for constituent percentages (M), with using fourteen, eleven, and five classes (M_{ref}) are very similar to Figure 5 and are not shown.

Inversion results for lithofacies inversions display various degrees of success. When sixteen facies classes were used, the inversion method was able to predict the gross lithology (e.g., dolomite or limestone) but failed to give detailed information about the facies (Figure 6). Especially, the inversion results for dolomite zones (see appendix for zone numbering) show the discrepancy between the core-derived and inverted facies. The lithofacies inversion for the case where fourteen classes were used shows slight improvement in the inverted facies results (Figure 7). Usage of eleven and five classes greatly improves the robustness of the facies inversion results (Figures 8, and 9). For Figure 8, it should be noted that petrophysically, there is no difference between class 3 and class 4 facies and class 10 and class 11 facies. These facies were described separately only on the basis of their textural differences as observed by petrographic analysis. Keeping this on mind, the inversion results using eleven facies classes were considered successful. Results when only five facies classes were used (Figure 9) show even a better agreement with the core-derived and inverted lithofacies. The inverted constituent percentages for each core using different a-priori geologic information, are very similar to each other and are not shown. The breaks in the core-derived values shown in blue, represent lack of data either due to missing core or missing petrographic information.

The inverted component percentages generally agree with percentages derived from petrographic analysis. Especially, dolomite, calcite, and porosity values, which are the main factors in defining a lithofacies, were correctly inverted (Figure 7). Inverted porosity shows good correlation with both Helium porosity and Neutron-Density cross plot porosity values regardless of the lithology in all cores. Anhydrite and shale inverted percentages generally agree with the core derived percentages except at few thin zones were they are overestimated. Overall, the tendency to overestimate shale is more common then the anhydrite. However, porosity seems not be effected by this inversion related miscalculation. For most depths, the amount of overestimation is less than 5-10%, with an exception of few thin zones where it reaches about 20%. The overestimation of anhydrite and shale is possibly due to the presence of other unaccounted minerals or inadequate inversion of component log parameters.

Figure 8 shows the lithofacies inversion results using sixteen original lithofacies classes. Inverted and core observed lithofacies curves generally mimic each other in shape but have different values. Inversion was able depict the general lithology, but in most dolomite cases, was unable deduce the specific lithofacies correctly. However, limestone intervals were mostly inverted to represent lithofacies similar to core-derived ones.

Figures 9 represents the results for lithofacies inversion using fourteen lithofacies classes. A-priori information contains two less facies less and the inverted and core-derived facies better agrees to each other where specific dolomite and limestone facies were better identified. Although, the inversion is improved a bit and general lithology is estimated with better success, the individual facies, especially in dolomite zones, are still not correctly identified. Percentages of the constituents show little difference from the previous inversion.

Lithofacies inversion using eleven facies classes yields significantly better correlation between inverted and core-derived lithofacies. Figure 10 shows that almost all of the inverted facies were similar to core-derived facies. Here it is important to again point out that, from petrophysical point of view, there is no difference between facies class 3 (sucrosic dolomite) and facies class 4 (dolomitized grainstone/packstone). These figures clearly show the success of the inversion, where majority of the dolomite facies were depicted correctly (either 3 or 4). Based on the success of the inversion in most of the dolomites, it is concluded that facies lor 2 were also correctly depicted as the low porosity non-reservoir dolomites zones. This observation is supported by the low porosity (both measured and inverted) zones coinciding with the zones of inverted facies of I and 2. Limestone zones showed similar success with the lithofacies inversion. Lagrange values used in the inversion were same as the previous trials and the inverted percentages showed very little difference than the earlier inversions.

The last lithofacies classification contains only five facies classes, and was used to test the depiction of any possible reservoir quality rocks. Figures 11 displays the plots of lithofacies inversion using only five facies classes as a-priori information. Lagrange values applied during the inversion, show very little change as well as the inverted constituent percentages. Lithofacies classification of inverted and core-derived facies mostly agree, except at some thin zones, which are usually low porosity dolomites.
Lithofacies inversion method, employing eleven facies classes could be a valuable tool in predicting facies when petrographic data is not comprehensive, or not available. A similar approach with few facies classes (possibly as reservoir vs non-reservoir) would depict gross lithologies, providing only minor information about individual facies. Such an approach would still be useful in eliminating unfavorable zones for production. If individual facies need to be depicted, a-priori geologic information is essential in defining various facies, which provide the basis of the comparison for various facies. Some of the facies classes used in the inversion method could have been grouped together to limit the number of facies. It is of course, preferred to depict as many facies as possible and the results of the lithofacies inversion utilizing eleven lithofacies classes covers the majority of the facies in the study cores.

To test the validity of the inversion method in the case of availability of one core only, the lithofacies inversion was conducted utilizing constituent parameters obtained from single core. Figure 10 is an example of such an inversion applied to core 2. Regardless of which core was used for constituent tool parameter inversion, there is little difference between the inverted lithofacies. It is concluded that the proposed lithofacies inversion method is applicable even if the input data is limited such as obtained from a single core only.

Based on the inversion results from five cores (one of them as a test core), the authors suggest that, lithofacies inversion can deduce valuable facies information about a reservoir provided that an adequate reference lithofacies classification is established. The degree of the facies information, that can be gathered depends on the reference lithofacies classification, in other words it depends on the a-priori geologic information. In general, the less classes are there, the better the correlation is between the inverted and observed lithofacies. The cut-off for number of facies classes used in the inversion depends on the degree of the precision sought by the inversion.

CONCLUSIONS

Depth shifting of cores, using classical methods, which employ the comparison of core derived logs and well logs may result in erroneous shifts. Application of synthetic logs, for the determination of depth shift could prove to be beneficial. The usage of synthetic logs provided critical information about the actual shift needed and revealed non-linear shifts for two of the cores. Detailed and correct depth shifting is especially important in carbonate reservoirs like Drinkard unit, where the best reservoir intervals are usually thin. The usage of synthetic logs, as a tool in determining the amount of necessary depth shift could benefit production in thin and/or alternating zones of reservoirs.

Establishment of a valid forward model for an inversion attempt, could provide petrophysical information about the logging parameters of the major constituents in the rocks. Such information can also be predicted by the application of synthetic logs.

An inversion algorithm utilizing a-priori geologic information can be used to deduce information about the lithofacies in the reservoir. Such an inversion can be used to correctly obtain information about percentages of constituents, which aid in providing the lithofacies information. The percentages of major minerals were depicted successfully with minor error, while the depiction of pore space is very precise in any lithology. The robustness of the inversion algorithm in depiction of lithofacies is directly related to the degree (resolution) of information sought. Generalized a-priori information with few lithofacies classes would reveal majority of the generalized lithofacies correctly but the specific

facies would be undetected. On the other hand, using too many lithofacies classifications in the inversion would harm the efforts for depicting specific facies. Overall, the robustness of the lithofacies is greatly affected by the information provided by the a-priori data. Where adequate a-priori information is provided, the inversion algorithm can reveal de tailed information about the lithofacies and can substitute for missing data (i.e., missing core).

The inversion results were able to reliable identify eleven different facies when detailed facies analysis was sought. It was also successful in depicting possible reservoir versus non-reservoir zones when the algorithm was limited to identify only five lithofacies. Inversion, using sixteen and fourteen different facies, showed to be a rel... tool in determining the gross lithology but in many cases failed to identify individual lithofacies.

In conclusion, an inversion algorithm that uses depositional facies knowledge from available cored wells as a-priori data, to refine the interpretation of the remaining wells would improve the correlation efforts and provide better understanding of the producing reservoir

ACKNOWLEDGEMENTS

This study was sponsored by Department of Geosciences and Honors College at Texas Tech University, Society of Professional Log Analysts, and Southwest Section of American Association of Petroleum Geologists.

APPENDIX

a) Lithofacies classification with sixteen lithofacies classes (percentages are averaged)

class #	dol %	ca %	anh %	sh %	por %
1	95.6	0	0	0	4.4
2	87.1	0	0	0	12.9
3	94.2	0	0	0	5.8
4	81.8	0	12.7	0	8.6
5	79.6	15.7	0	0	4.7
6	85.3	0	0	3.9	10.6
7	85.9	0	0	0	14.2
8	78.7	3.1	12.7	0.0	8.6
9	84.8	7.7	0	0	7.5
10	23	72.2	0	0	4.8
11	27.3	66.5	0	3.5	2.6
12	0	94.7	0	0	5.3
13	0	88.5	0	0	11.5
14	0	82.4	0	0	17.6
15	0	69.5	15	0	15.5
16	0	94	0	3.5	2.5

Class 1: Mosaic Dolomite
Class 2: Sucrosic Dolomite, Bimodal Sucrosic Dolomite
Class 3: Closely packed Sucrosic Dolomite
Class 4: Anhydritic Sucrosic Dolomite
Class 5: Calcite plugged Sucrosic Dolomite
Class 6: Very fine crystalline Sucrosic Dolomite, Very fine crystalline Dolomite
Class 7: Dolomitized Pelleoidal Skeletal Grainstone, Dolomitized Skeletal Pelleoidal Grainstone, Dolomitized Pelleoidal Skeletal Packstone, Dolomitized Skeletal Pelleoidal Packstone, Dolomitized Pelleoidal Packstone
Class 8: Anhydritic Dolomitized Pelleoidal Packstone
Class 9: Dolomitized Pelleoidal Skeletal Wackestone, Dolomitized Skeletal Pelleoidal Wackestone, Dolomitized Pelleoidal Wackestone, Dolomitized Mudstone
Class 10: Dolomitic Pelleoidal Skeletal Grainstone, Dolomitic Skeletal Pelleoidal Grainstone Dolomitic

Skeletal Pelleoidal Packstone, Dolomitic Pelleoidal Skeletal Packstone, Dolomitic Skeletal Packstone

Class 11: Dolomitic Pelleoidal Skeletal Wackestone, Dolomitic Skeletal Pelleoidal Wackestone, Dolomitic Skeletal Wackestone, Dolomitic Mudstone, Dolomitic Skeletal Mudstone

Class 12: Pelleoidal Skeletal Grainstone, Pelleoidal Grainstone, Pelleoidal Skeletal Grainstone, Pelleoidal Skeletal Packstone, Skeletal Pelleoidal Packstone

Class 13: Oolithic Pelleoidal Grainstone, Oolithic Grainstone

Class 14: Oomoldic Grainstone, Oomoldic Packstone

Class 15: Anhydritic Oomoldic Grainstone

Class 16: Skeletal Pelleoidal Wackestone, Pelleoidal Skeletal Wackestone, Mudstone, Pelleoidal Skeletal Mudstone

b) Lithofacies classification with fourteen lithofacies classes

class #	dol %	ca %	anh %	sh %	por %
1	95.6	*0*	0	0	4.4
2	94.2	0	0	0	5.8
3	81	12.2	0	0	6.8
4	79.9	0	11.2	0	8.9
5	85.3	0	0	3.9	10.6
6	87.1	0	0	0	12.9
7	85.9	0	0	0	14.2
8	23	72.2	0	0	**4.8**
9	27.3	66.5	0	3.5	2.6
10	*0*	94.7	0	0	5.3
11	*0*	88.5	0	0	11.5
12	*0*	82.4	0	0	17.6
13	*0*	69.5	15	0	15.5
14	*0*	94	0	3.5	2.5

Class 1: Mosaic Dolomite

Class 2: Closely packed Sucrosic Dolomite

Class 3: Dolomitized Pelleoidal Skeletal Wackestone, Dolomitized Skeletal Pelleoidal Wackestone, Dolomitized Pelleoidal Wackestone, Dolomitized Mudstone, Calcite plugged Sucrosic Dolomite

Class 4: Anhydritic Sucrosic Dolomite, Anhydritic Dolomitized Pelleoidal Packstone

Class 5: Very fine crystalline Sucrosic Dolomite, Very fine crystalline Dolomite

Class 6: Sucrosic Dolomite, Bimodal Sucrosic Dolomite

Class 7: Dolomitized Pelleoidal Skeletal Grainstone, Dolomitized Skeletal Pelleoidal Grainstone, Dolomitized Pelleoidal Skeletal Packstone, Dolomitized Skeletal Pelleoidal Packstone, Dolomitized Pelleoidal P

Class 8: Dolomitic Pelleoidal Skeletal Grainstone, Dolomitic Skeletal Pelleoidal Grainstone Dolmitic Skeletal Pelleoidal Packstone, Dolomitic Pelleoidal Skcltal Packstone. Dolemitic Skeletal Pakcstone

Class 9: Dolomitic Pelleoidal Skeletal Wackestone, Dolomitic Skeletal Pelleoidal Wackestone, Dolomitic Skeletal Wackestone, Dolomitic Mudstone, Dolomitic Skeletal Mudstone Packstone

Class 10: Pelleoidal Skeletal Grainstone, Pelleoidal Grainstone, Pelleoidal Skeletal Grainstone, Pelleoidal Skeletal Packstone, Skeletal Pelleoidal Packstone

Class 11: Oolithic Pelleoidal Grainstonc, Oolithic Grainstone,

Class 12: Oomoldic Grainstone, Oomoldic Packstonc

Class 13: Anhydritic Oomoldic Grainstone

Class 14: Skeletal Pelleoidal Wackestone, Pelleoidal Skeletal Wackstone, Mudstone, Pelleoidal Skeletal Mudstone

c) Lithofacies classification with eleven lithofacies classes

class #	dol %	ca %	anh %	sh %	por %
1	95.6	0	0	0	4.4
2	94.2	0	0	0	5.8
3	86.7	0	0	0.8	12.4
4	85.8	0	0	0	14.2
5	23	72.2	0	0	4.8
6	27.3	66.5	0	3.5	2.6
7	0	88.5	0	0	11.5
8	0	69.5	15	0	15.5
9	0	82.4	0	0	17.6
10	0	94.7	0	0	5.3
11	0	94	0	3.5	2.5

Class 1: Mosaic Dolomite
Class 2: Closely packed Sucrosic Dolomite, Dolomitized Pelleoidal Skeletal Wackestone, Dolomitized Skeletal Pelleoidal Wackestone, Dolomitized Pelleoidal Wackestone, Dolomitized Mudstone,
Class 3: Sucrosic dolomite, Very fine crystalline Sucrosic Dolomite, Very fine crystalline Dolomite
Class 4: Dolomitized Pelleoidal Skeletal Grainstone, Dolomitized Skeletal Pelleoidal Grainstone, Dolomitized Pelleoidal Skeletal Packstone, Dolomitized Skeletal Pelleoidal Packstone, Dolomitized Pelleoidal Packstone
Class 5: Dolomitic Pelleoidal Skeletal Grainstone, Dolomitic Skeletal Pelleoidal Grainstone Dolomitic Skeletal Pelleoidal Packstone, Dolomitic Pelleoidal Skeletal Packstone, Dolomitic Skeletal Packstone
Class 6: Dolomitic Pelleoidal Skeletal Wackestone, Dolomitic Skeletal Pelleoidal Wackestone, Dolomitic Skeletal Wackestone, Dolomitic Mudstone, Dolomitic Skeletal Mudstone
Class 7: Oolithic Pelleoidal Grainstone, Oolithic Grainstone
Class 8: Anhydritic Oomoldic Grainstone
Class 9: Oomoldic Grainstone, Oomoldic Packstone
Class 10: Pelleoidal Skeletal Grainstone, Pelleoidal Grainstone, Pelleoidal Skeletal Grainstone, Pelleoidal Skeletal Packstone, Skeletal Pelleoidal Packstone, Oolithic Pelleoidal Grainstone, Oolithic Grainstone
Class 11 Skeletal Pelleoidal Wackestone, Pelleoidal Skeletal Wackestone, Mudstone, Pelleoidal Skeletal Mudstone

d) Lithofacies classification with five lithofacies classes

class#	dol %	ca %	anh %	sh %	por %
1	94.9	0	0	0	5.1
2	86.5	0	0	0.6	12.9
3	25.6	67	0.6	3.4	3.5
		.8	0	0	15.2
5	0	94.4	0	1.8	3.9

Class 1: Dolomite (Non-reservoir quality)
Class 2: Dolomite (Reservoir quality)
Class 3: Dolomitic limestone (Non-reservoir quality)
Class 4: Limestone (Reservoir quality)
Class 5: Limestone (Non-reservoir quality)

REFERENCES

Davis, J.C. (1986), Statistics and Data Analysis in Geology, 2nd ed. John Wiley and Sons, New York, 646 pp.

Doveton, J. H. (1994), Geologic Log Analysis Using Computer Methods, AAPG Computer Applications in Geology No.2, Tulsa, AAPG, p. 47-64.

Doveton, J. H., and Cable, H. W. (1979), Fast matrix for the lithological interpretation of geophysical logs, *In* Gill, D., and Meriam, D.F., eds., Geomathematical and Petrophysical Studies in Sedimentology: Oxford, Pergamon Press, p.101-116.

Dunham, R.J. (1962), Classification of carbonate rocks according to depositional texture. In W.E. Ham (ed.), Classifi cation of Carbonate Rocks, pp. 108-121. AAPG Mem. No. 1.

Gurrola, H., Baker, E. G., and Minster, B.J. (1995), Simultaneous time domain deconvolution with Application to the computation of receiver functions, Geophys. Jour. Int., v. 120, 537-543.

Halliburton (1994), Halliburton Log Interpretation Charts, Halliburton Energy Services Houston, Texas.

Hoffman, J. D. (1992), Numerical Methods for Engineers and Scientists, McGraw Hill, p. 32-35.

Ruppel, S.C., Kerans, C., Major, R.P., and Holtz, M.H. (1995), Controls on reservoir heterogeneity in Permian shallow-water-platform carbonate reservoirs, Permian Basin: Implications for improved recovery. Bureau of Economic

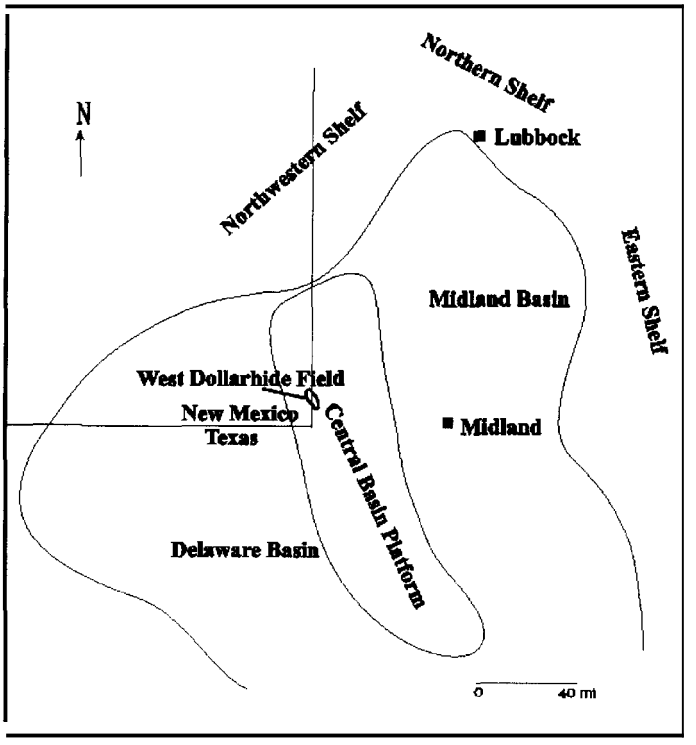

Figure 1 - Generalized Map of the Permian Basin and Location of West Dollarhide Field (modified from Ruppel and others, 1995)

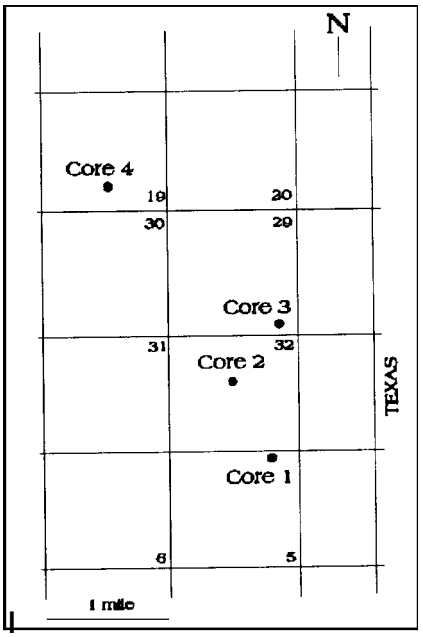

Figure 2 - Location of the Four Studied Cores in the West Dollarhide Field, Lea County, New Mexico (modified from Johnson, 1999)

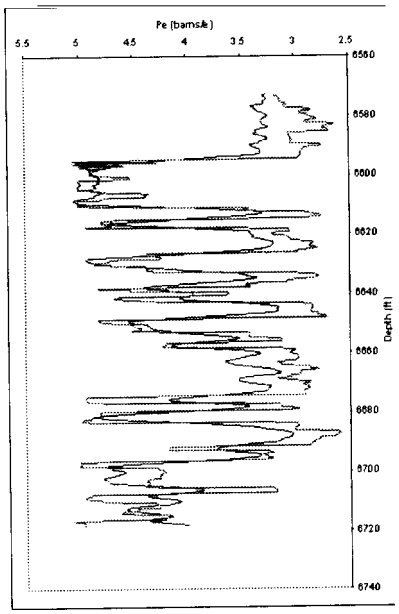

Figure 3 - Plots of Calculated (synthetic) Pe Log and Measured Pe Log for Core 3

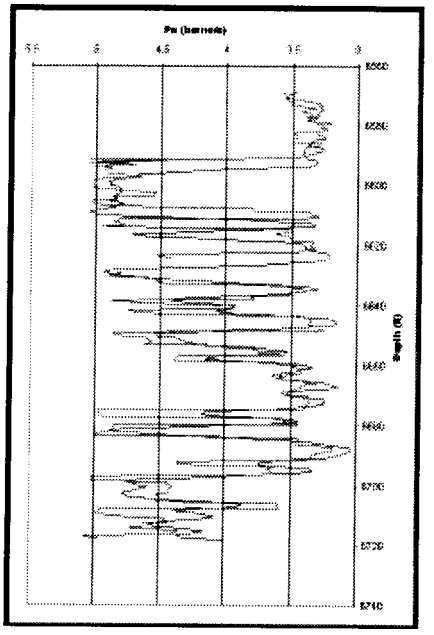

Figure 4 - Plots of Calculated (synthetic) Pe Log and Measured Pe Log for Core 3 Using Unmodified Depth Shift

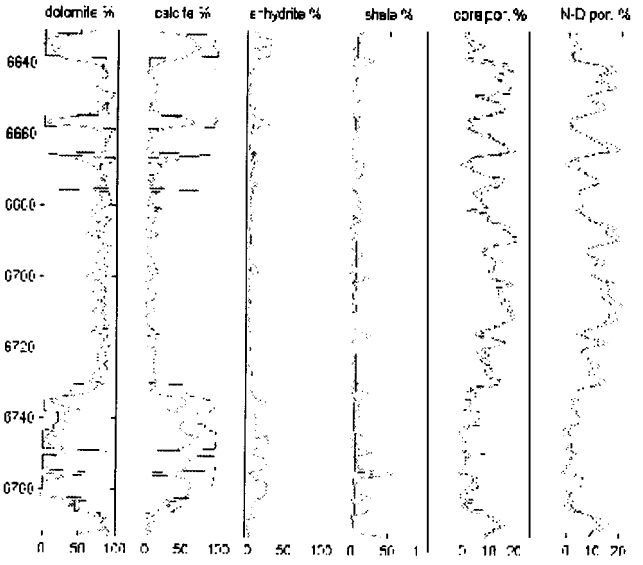

Figure 5 - Inverted and Core Derived Percentages for Core 4

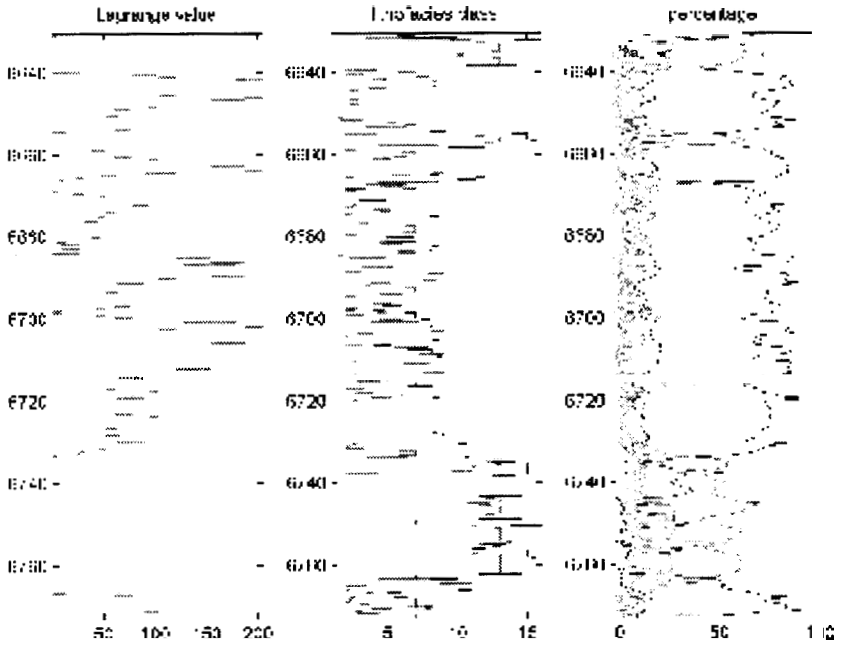

Figure 6 - Inversion Results for Core **4** Using Sixteen Lithofacies Classes

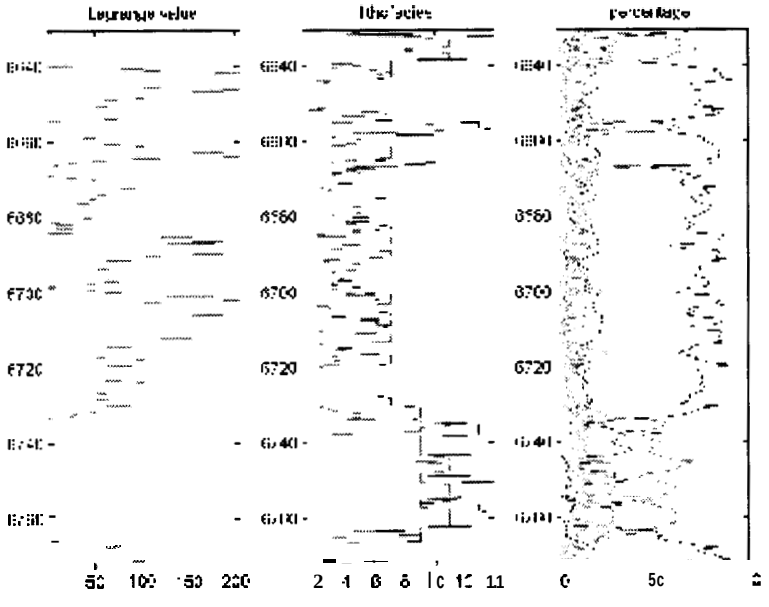

Figure 7 - Inversion Results for Core **4** Using Fourteen Lithofacies Classes

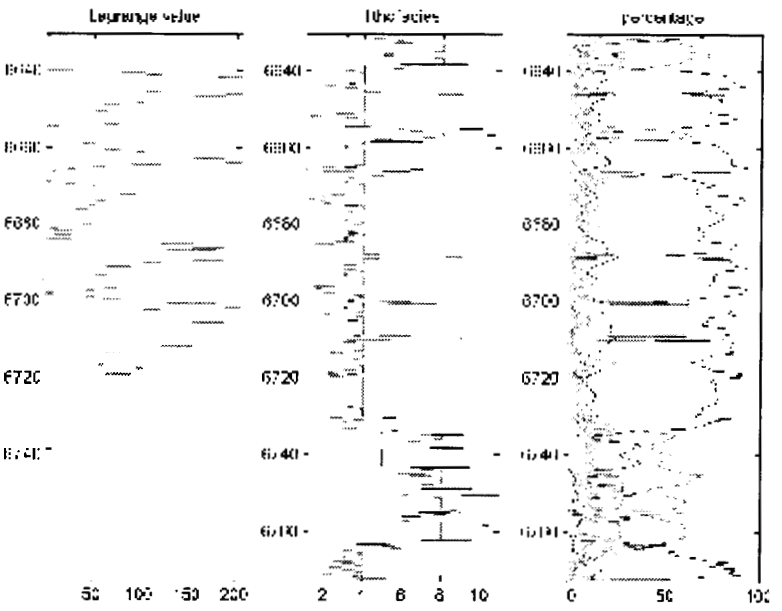

Figure 8 - Inversion Results for Core **4** Using Eleven Lithofacies Classes

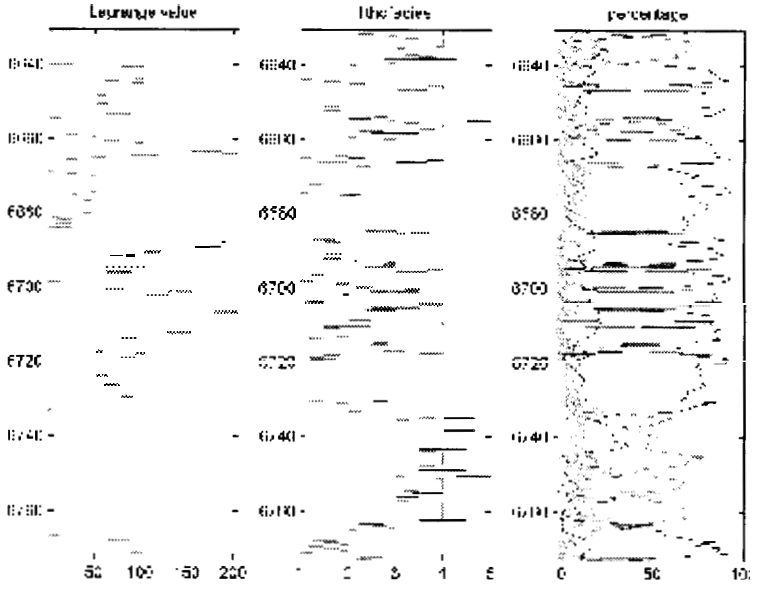

Figure 9 - Inversion Results for Core **4** Using Five Lithofacies Classes

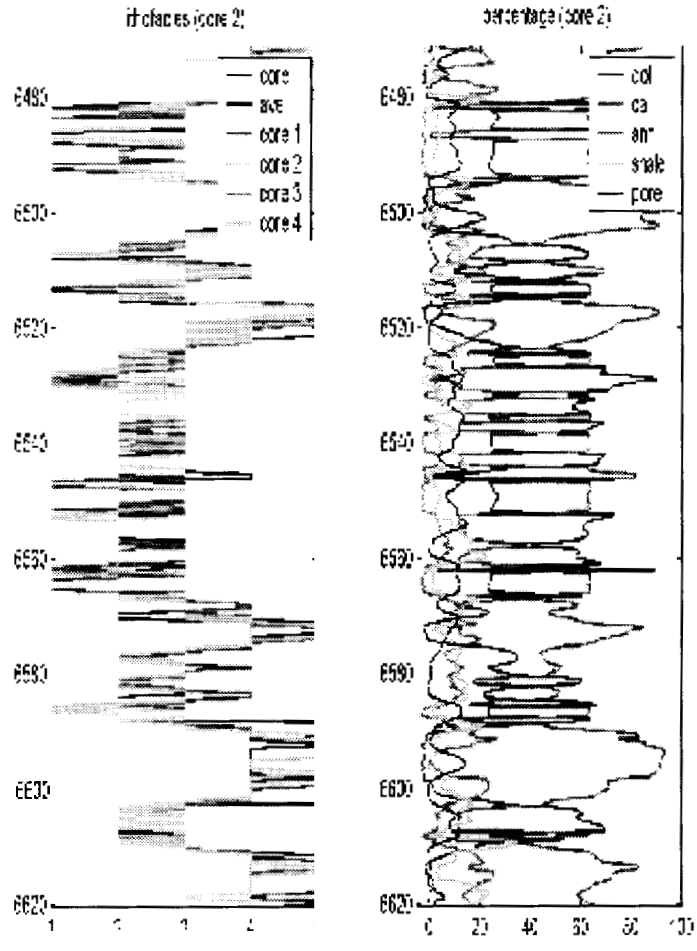

Figure 10 - Lithofacies Inversion Applied to Core 2 By Using Various Inverted Constituent Tool Parameters (i.e. Core 2 refers to parameters obtained from Core 2 only. Average is the average value for all cores.) Percentage plot applies only the average constituent tool parameters.